Fabrication of Biodegradable Poly(lactic acid) Particles in Flow-focusing Glass Capillary Devices

G.T. Vladisavljević[1], J.V. Henry[1], W.J. Duncanson[2], H.C. Shum[3], D.A. Weitz[2]
[1]*Department of Chemical Engineering, Loughborough University, Loughborough, LE11 3TU, UK;* [2]*Department of Physics, Harvard University, Cambridge, MA 02138, USA;*
[3]Department of Mechanical Engineering, University of Hong Kong, Hong Kong.

Abstract

Monodisperse poly(dl-lactic acid) (PLA) particles with a diameter in the range from 12 to 100 μm were fabricated in flow focusing glass capillary devices by evaporation of dichloromethane (DCM) from emulsions at room temperature. The dispersed phase was 5% (w/w) PLA in DCM containing a small amount of Nile red and the continuous phase was 5% (w/w) poly(vinyl alcohol) in reverse osmosis water. Particle diameter was 2.7 times smaller than the size of the emulsion droplet template indicating that the particle porosity was very low. SEM images revealed that the majority of particle pores are in the sub-micron region but in some instances these pores can reach 3 μm in diameter. Droplet diameter was influenced by the flow rates of the two phases and the entry diameter of the collection capillary tube; droplet diameters decreased with increasing values of the flow rate ratio of the dispersed to continuous phase to reach constant minimum values at 40-60 % orifice diameter. At flow rate ratios less than 5, jetting can occur, giving rise to large droplets formed by detachment from relatively long jets (~10 times longer than droplet diameter).

Key words: Flow Focusing Microfluidics · Poly(lactic Acid) Particle · Monodisperse Particles · Glass Capillary Device · Emulsification/Solvent Evaporation

1 Introduction

Microspheres composed of biodegradable polymers have been used for the encapsulation and controlled release of hydrophilic and hydrophobic drugs [1], ultrasound and molecular imaging [2], cell cultivation in tissue engineering [3], fabrication of scaffolds for bone tissue repair applications [4], fabrication of composite coatings for implantable devices [5], etc. The most commonly used biodegradable synthetic polymers for these applications are poly(lactic acid), PLA, and poly(lactic-co-glycolic) acid, PLGA, since they both have favourable properties such as good biocompatibility, biodegradability, and mechanical strength [1,6].

* Corresponding Author: Goran Vladisavljević, e-mail: G.Vladisavljevic@lboro.ac.uk

PLA particles are usually produced via single emulsion route shown in Fig. 1(a). In this process, a mixture of PLA and volatile organic solvent is emulsified in the aqueous surfactant solution. The second step involves solvent evaporation or extraction, resulting in shrinkage of the droplets and formation of a coherent solid particle as shown in Figure 1(b). These particles are suitable for encapsulation of hydrophobic drugs [7].

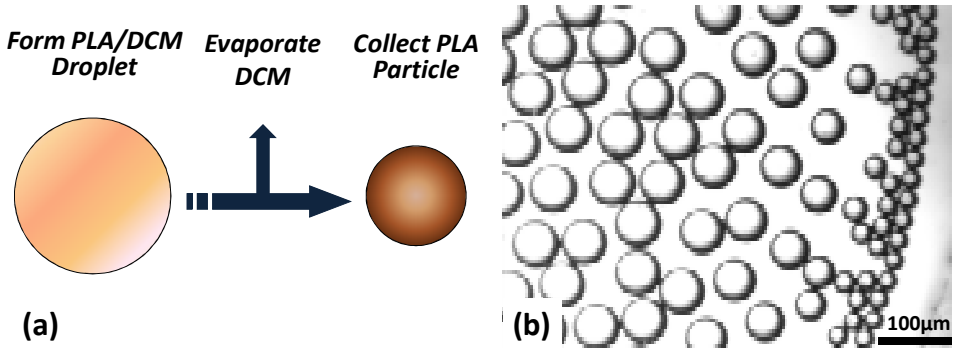

Figure 1 Emulsion templating method for producing PLA microparticles. (a) Schematic diagram of process; (b) micrograph of emulsions undergoing DCM evaporation.

The PLA droplets shrank during solvent (DCM) evaporation, as demonstrated in Figure 1(b). In this figure the average emulsion droplet diameter was 64 µm and the resulting particle diameter (at the right-hand edge of Fig. 1(b)) was 24 µm, which agrees well with theoretical value of 64/2.7 = 24 µm calculated on the assumption of complete solvent evaporation and zero particle porosity.

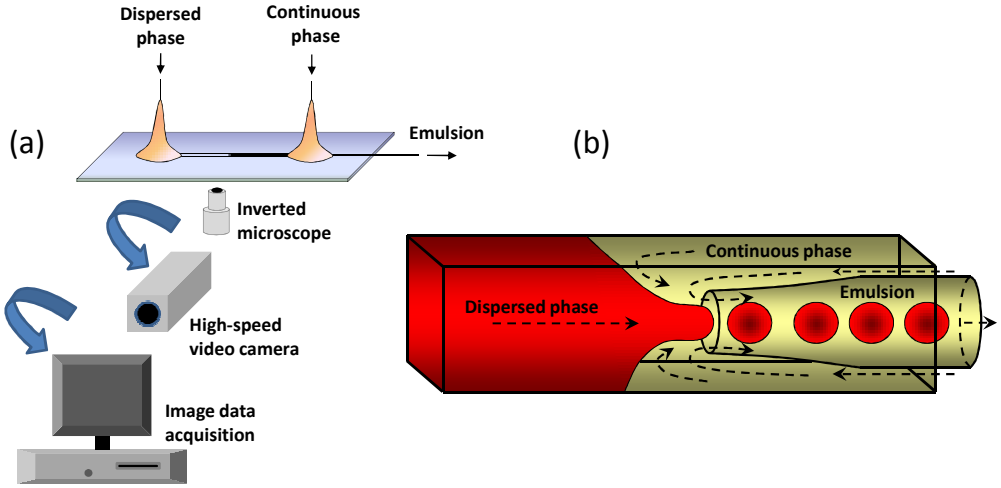

Figure 2 Experimental setup for the two-phase flow in a flow focusing configuration. (a) visual representation of data collection; (b) enlarged view of flow focusing zone in device, where droplets are formed.

Precision generation of drops is a crucial step in fabrication of PLA particles because monodisperse particles can only be produced from monodisperse droplets. Conventional methods for production of PLA particles based on spray drying [8] or homogenization in a stirred vessel or high-pressure homogenizers result in polydisperse particles. For

example, Straub et al. [8] have produced PLGA particles with a mean size of 2.3 μm using a spray dryer at 20 mL min^{-1} emulsion flow rate, but the particle size in the product was in the range between 1 and 10 μm. Monodisperse particles are favourable in drug delivery and ultrasound imaging applications, because particles behave homogenously, ensuring a predictable release rate profile and acoustic response. Several drop-by-drop methods have been used in production of PLA and PLGA microspheres, such as ink-jet printing [9], direct and pre-mix membrane emulsification [7-10], extrusion through a nozzle under acoustic excitation [11] and flow focusing in PDMS microfluidic devices [12]. However, these methods either produce particles with high coefficient of variations or are expensive to build and to operate. For example, coefficient of variations of particle sizes for PLGA particles produced by direct membrane emulsification was 7–16% [8]. Using repeated pre-mix membrane emulsification, the mean particle size of around 1 μm was achieved but the span of size distribution was 0.7 [10]. The purpose of this study is to fabricate inexpensive glass capillary devices, developed by Utada et al. [13], shown in Figure 2, so that highly uniform PLA microspheres may be produced economically.

2 Materials and Methods

Glass capillaries of inner diameter 580 μm and outer diameter 1 mm were pulled using a Sutter Instruments model P-97 micropipette puller to obtain a tapered tip. Each tip was sanded smooth to obtain an orifice with an entry diameter of 60–280 μm, followed by surface modification with 2-[methoxy(polyethylenoxy)propyl]trimethoxysilane (Gelest Inc.). These capillaries with hydrophilic coating were then inserted and glued in the centre of a square glass tube (AIT Inc.) of 1.05 mm inner dimension. The oil phase was 5 % (w/w) poly(dl-lactic acid) (Polysciences Europe GmbH, molecular weight = 15,000 g mol^{-1}) in dichloromethane (DCM) containing small amount of Nile red dye (Sigma-Aldrich). The role of dye in our preparation was to easily observe the position of the interface between the organic and aqueous phase in the device because Nile red is insoluble in water. The viscosity and density of the organic phase is 0.3631 mPa·s and 1.31 kg·dm^{-3} respectively at 298K. The aqueous phase was 5 % (w/w) polyvinyl alcohol (Sigma-Aldrich, 87-89% hydrolyzed) in Milli-Q water. The interfacial tension between the two phases was measured as 2.26 mN/m using a Krüss DSA-100 pendant drop tensiometer. The both phases were delivered to the device from gas tight syringes using separate Harvard Apparatus PHD 22/2000 syringe pumps connected to 19-gauge needles, as shown in Figure 2(a).

Flow optimization (through manually reprogramming flow rates of both phases) was enabled by real-time visualization of emulsion formation using Phantom V5.1 high-speed

camera focused by an inverted microscope. The images are obtained using high-speed video footage at 1000–2000 frames per second. Droplet diameters were measured using ImageJ v.1.44 software. Frames of the high-speed video footage were taken to allow individual measurement of the droplet diameters. Using this technique also, stills were studied to characterize the drop generation behavior and estimate drop generation rate.

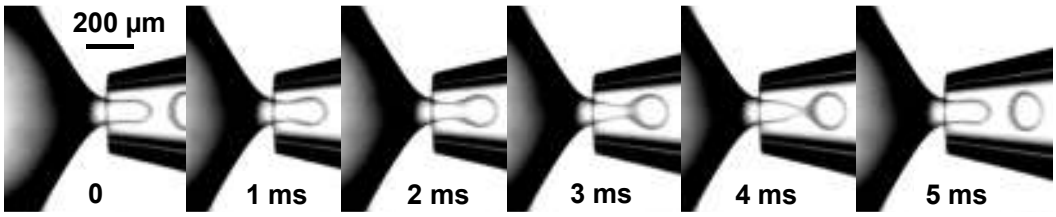

Figure 3 Six consecutive frames of droplet production via dripping mechanism over the course of 5 ms. The drop generation frequency was 206 Hz.

Examples of the video footage gathered at 1000 fps are shown in Figure 3. In this experiment, the flow rate of the dispersed phase, Q_d was set at 1.5 ml·h^{-1}, the flow rate of the continuous phase, Q_c, was set at 13 ml·h^{-1} and the resulting observed diameter of the droplets was d = 156 µm. The following mass balance equation can be used for the dispersed phase: $f = Q_d/(d^3\pi/6)$, where f is the frequency of drop generation. Putting d = 1.56×10^{-4} m and $Q_d = 4.17\times10^{-10}$ m^3/s into the above equation, one obtains 210 Hz which is in good agreement with 206 Hz estimated from the video recordings.

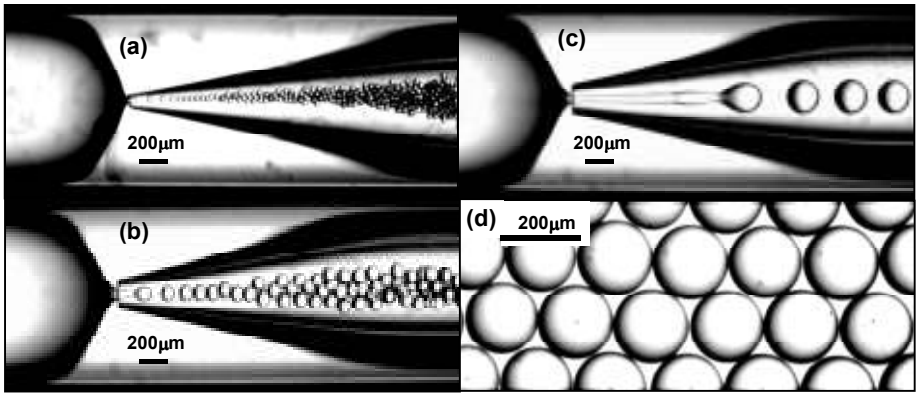

Figure 4 Images of droplet formation under varying flow rates and orifice size. (a) Q_c = 0.5 ml·h^{-1}, Q_d = 0.003 ml·h^{-1}, $d_{orifice}$ = 60 µm, d = 33 µm; (b) Q_c =5 ml·h^{-1}, Q_d = 1 ml·h^{-1}, $d_{orific\ e}$ = 130 µm, d = 100 µm; (c) Q_c = 6.5 ml·h^{-1}, Q_d = 0.7 ml·h^{-1}, $d_{orifice}$ = 130 µm, d = 230 µm; (d) collected monodisperse droplets.

The fluid flow rates and device geometry has an important effect on droplet size, as illustrated by the examples in Fig. 4. In (a), the orifice size was made very small so as to obtain relatively small droplets with a diameter of 33 µm that can be converted into 12 µm particles after solvent evaporation. In (b) and (c) the device was the same but the flow rates were different, leading to different droplet formation regimes. As can be seen in (d)

collected droplets are packed into regular hexagonal arrangements, evidence of a high degree of monodispersity, with a coefficient of variation of less than 2%.

In Figure 5, the relationship between the dimensionless droplet diameter, $d/d_{orifice}$ and flow rate ratio, Q_c/Q_d is shown. There are two different regimes of droplet formation, e.g. jetting and dripping. At low flow rate ratios, where $Q_c/Q_d < 5$ jetting can occur, which gives rise to large droplets and relatively long length jets prior to droplet detachment. At jetting, jet lengths are ~10 times longer than droplet diameter and the droplet diameter can be up to twice the diameter of the orifice. In addition, droplets formed under jetting regime are more polydisperse than droplets formed under dripping regime. These regimes are commutative at Q_c/Q_d <5, and any small disturbance received by the system may either cause or destroy long jetting breakup. The second feature of Figure 5 is that droplet diameters decrease with increasing values of Q_c/Q_d to reach their respective minimum values at 40-60 % orifice diameter. At flow rate ratios between 5 and 15, droplets have the highest degree of monodispersity. At $Q_c/Q_d > 15$, a second region of droplet formation from extended jetting predominates; these extensional flows however, are not as long as those encountered at $Q_c/Q_d < 5$, nor as wide as those exhibited at these values; for this reason are not subject to the same instability, but instead exhibit a tip streaming regime, which is reflected in the smaller, more polydisperse droplet diameters.

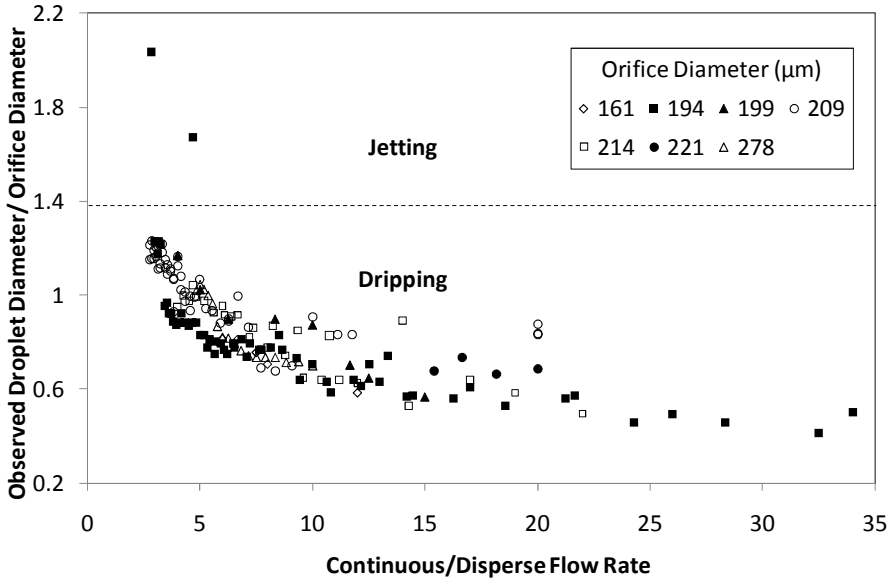

Figure 5 Graph of droplet diameter/orifice diameter vs. flow rate ratio, Q_c/Q_d, for a range of device internal orifice diameters: ◊ = 161 µm; ■ = 194 µm; ▲= 199 µm; o = 209 µm; □ = 214 µm; ● = 221 µm; Δ = 278 µm.

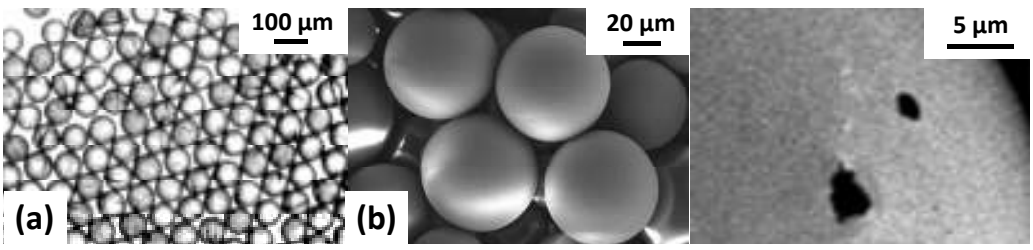

Figure 6 (a) Optical micrograph of 84 μm poly(lactic) acid particles; (b) Scanning Electron Micrograph of 63 μm particles; (c) Surface of a PLA particle showing two micrometer-sized pores.

The polylactic acid particles have a high degree of monodispersity and low degrees of attrition and porosity, as shown in the optical and electron microscope images in Fig. 6. The coefficient of variation of particle sizes in Fig. 6(a) is 2.3%. Examination of SEM images has revealed that the surface of PLA particles was essentially non-porous with a majority of pores in the sub-micron region but in some rare instances these pores can reach 3 μm in diameter, as shown in Fig. 6(c).

Conclusions

The diameter of PLA/DCM droplets in flow focusing glass capillary devices has been closely controlled by phase flow rates and entry diameter of collection capillary tube. The maximum emulsion and particle monodispersity was achieved at flow rate ratios of continuous to dispersed phase between 5 and 15; outside of this range, jetting during the formation of emulsion droplets predominates, and is accompanied by more polydisperse and for lower flow rate ratios, larger droplet diameters. Particle diameters have been established to be 2.7 times smaller than the emulsion diameters. The resultant particles have low porosity, and are highly monodisperse.

Acknowledgment

The work was supported by the Engineering and Physical Sciences Research Council (EPSRC) of the United Kingdom (grant reference number: EP/HO29923/1).

References

[1] J.A. Jain, Biomaterials **21**, 2475 (2000).

[2] H. Sawalha, K. Schroën, R. Boom, Chem. Eng. J. **169**, 1 (2011).

[3] A.L. Klibanov, J. Nucl. Cardiol. **14**, 876 (2007).

[4] X. Shi, L. Sun, J. Jiang, X. Zhang, W. Ding, Z. Gan, Macromol. Biosci. **9**, 1211 (2009).

[5] Y. Wang, X. Shi, L. Ren, C. Wang, D.A. Wang, Mat. Sci. Eng. C **29**, 2502 (2009).

[6] U. Bhardwaj, F. Papadimitrakopoulos, D.J. Burgess, J. Diabetes Sci. Technol. **2**, 1016 (2008).

[7] F. Ito, K. Makino, Colloid. Surf. B **39**, 17 (2004).

[8] J.A. Straub, D.E. Chickering, C.C. Church, B. Shah, T. Hanlon, H. Bernstein, J. Control Release **108**, 21 (2005).

[9] M.R. Böhmer, R. Schroeders, J.A.M. Steenbakkers, S.H.P.M. de Winter, P.A. Duineveld, J. Lub, W.P.M. Nijssen, J.A. Pikkemaat, H.R. Stapert, Colloid. Surf. A **289**, 96 (2006).

[10] H.Sawalha, N. Purwanti, A. Rinzema, K. Schroën, R. Boom, J. Membr. Sci. **310**, 484 (2008).

[11] C. Berkland, K.K. Kim, D.W. Pack, J. Control. Release **73**, 59 (2001).

[12] Q. Xu, M. Hashimoto, T.T. Dang, T. Hoare, D.S. Kohane, G.M. Whitesides, R. Langer, D.G. Anderson, Small **5**, 1575 (2009).

[13] A.S. Utada, L.-Y. Chu, A. Fernandez-Nieves, D.R. Link, C. Holtze, D.A. Weitz, MRS Bull. **32**, 702 (2007).

Figure legends

Figure 1 Emulsion templating method for producing PLA microparticles. (a) Schematic diagram of process; (b) micrograph of emulsions undergoing DCM evaporation.

Figure 2 Experimental setup for the two-phase flow in a flow focusing configuration. (a) visual representation of data collection; (b) enlarged view of flow focusing zone in device, where droplets are formed.

Figure 3 Four consecutive frames of droplet production via dripping mechanism over the course of 1.5 ms.

Figure 4 Images of droplet formation under varying flow rates and orifice size. (a) Q_c= 0.5 ml·h^{-1}, Q_d= 0.003 ml·h^{-1}, $d_{orifice}$= 60 μm, $d_{droplet}$= 33 μm; (b) Q_c=5 ml·h^{-1}, Q_d= 1 ml·h^{-1}, $d_{orifice}$=130 μm, $d_{droplet}$= 100 μm; (c) Q_c=6.5 ml·h^{-1}, Q_d=0.7 ml·h^{-1}, $d_{orifice}$=130 μm, $d_{droplet}$=230 μm; (d) collected monodisperse droplets.

Figure 5 Graph of droplet diameter/orifice diameter vs. flow rate ratio, Q_c/Q_d, for a range of device internal orifice diameters: ◊ = 161 μm; ■ = 194 μm; ▲= 199 μm; o = 209 μm; □ = 214 μm; ● = 221 μm; Δ = 278 μm.

Figure 6 (a) Optical micrograph of 84 μm poly(lactic) acid particles; (b) Scanning Electron Micrograph of 63 μm particles; (c) Surface of a PLA particle showing two micrometer-sized pores.

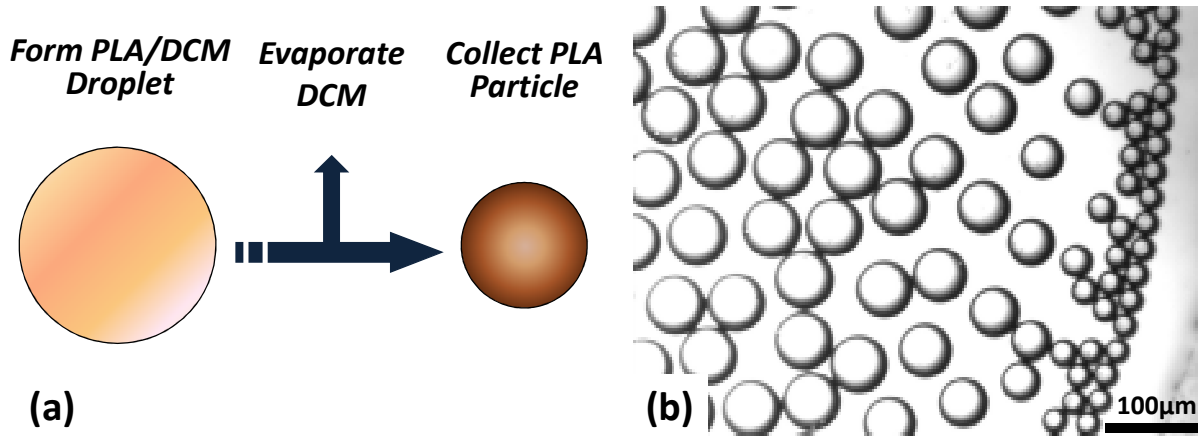

Figure 1 Emulsion templating method for producing PLA microparticles. (a) Schematic diagram of process; (b) micrograph of emulsions undergoing DCM evaporation.

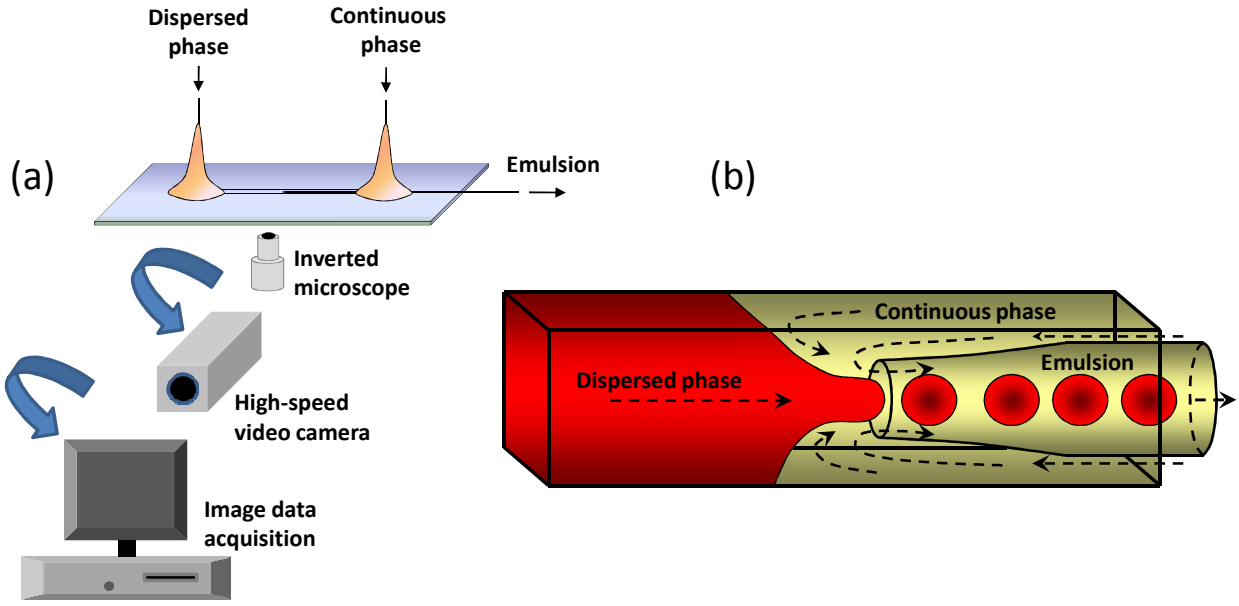

Figure 2 Experimental setup for the two-phase flow in a flow focusing configuration. (a) visual representation of data collection; (b) enlarged view of flow focusing zone in device, where droplets are formed.

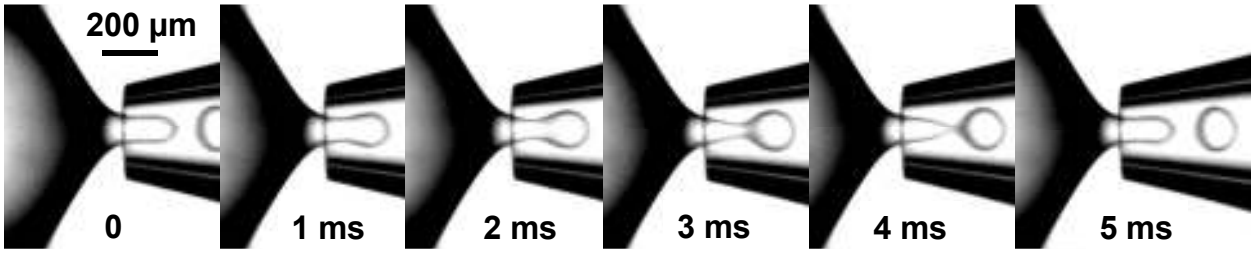

Figure 3 Six consecutive frames of droplet production via dripping mechanism over the course of 5 ms. The drop generation frequency was 206 Hz.

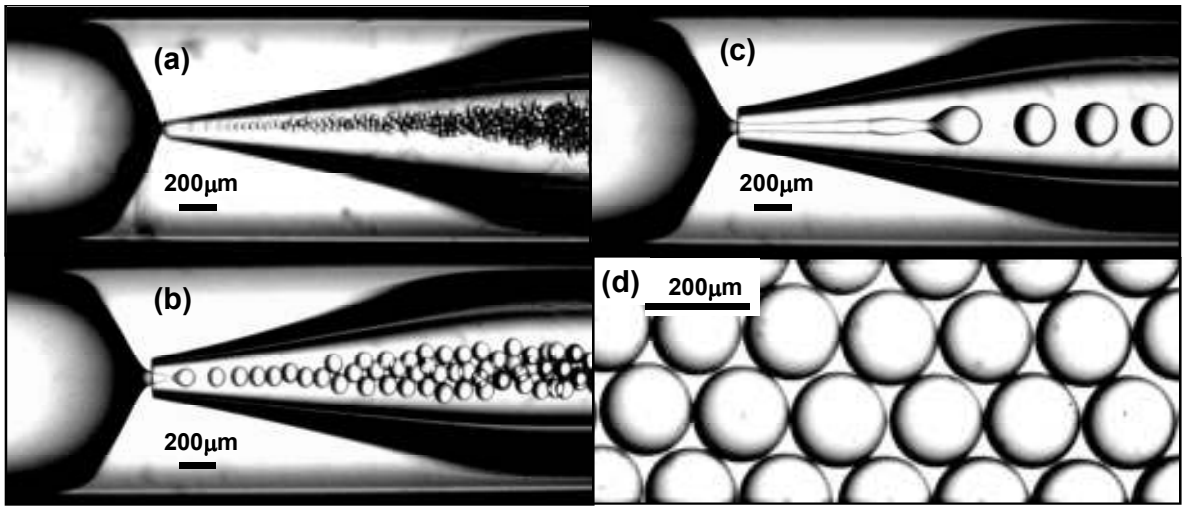

Figure 4 Images of droplet formation under varying flow rates and orifice size. (a) Q_c = 0.5 ml·h^{-1}, Q_d = 0.003 ml·h^{-1}, $d_{orifice}$ = 60 μm, d = 33 μm; (b) Q_c =5 ml·h^{-1}, Q_d = 1 ml·h^{-1}, $d_{orific\ e}$ = 130 μm, d = 100 μm; (c) Q_c = 6.5 ml·h^{-1}, Q_d = 0.7 ml·h^{-1}, $d_{orifice}$ = 130 μm, d = 230 μm; (d) collected monodisperse droplets.

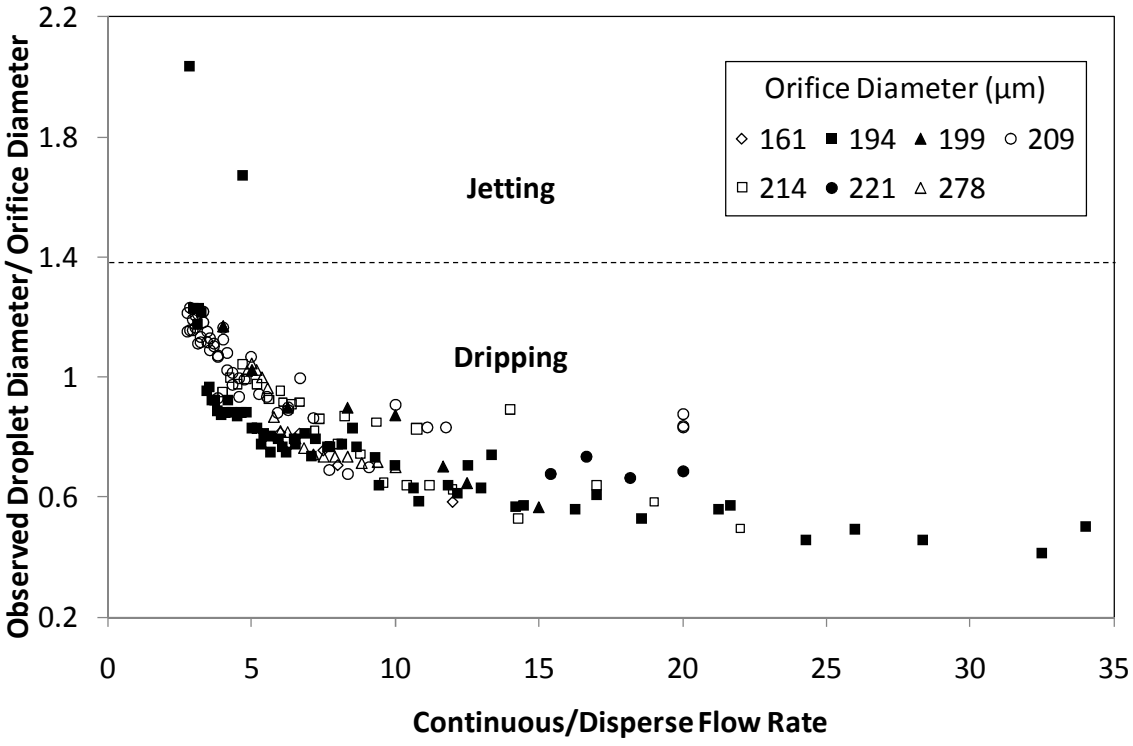

Figure 5 Graph of droplet diameter/orifice diameter vs. flow rate ratio, Q_c/Q_d, for a range of device internal orifice diameters: ◊ = 161 µm; ■ = 194 µm; ▲= 199 µm; o = 209 µm; □ = 214 µm; ● = 221 µm; Δ = 278 µm.

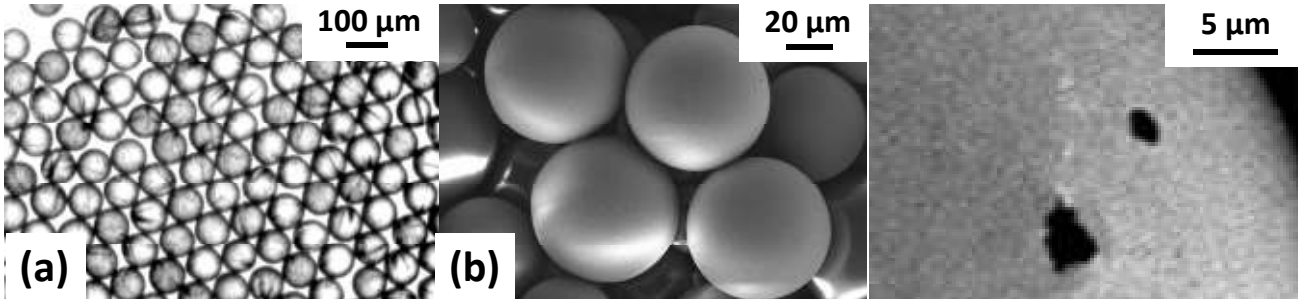

Figure 6 (a) Optical micrograph of 84 µm poly(lactic) acid particles; (b) Scanning Electron Micrograph of 63 µm particles; (c) Surface of a PLA particle showing two micrometer-sized pores.